EXAFS and X-Ray Diffraction Studies on the Structure of the Tetrathiocyanatocadmate(II) Complex in Dimethyl Sulfoxide

Kazuhiko Ozutsumi,* Toshiyuki Takamuku,† Shin-ichi Ishiguro,† and Hitoshi Ohtaki*,††

Department of Chemistry, University of Tsukuba, Tsukuba 305
†Department of Electronic Chemistry, Tokyo Institute of Technology at Nagatsuta, Midori-ku, Yokohama 227
††Coordination Chemistry Laboratories, Institute for Molecular Science, Myodaiji, Okazaki 444

(Received February 20, 1992)

The structure of the tetrathiocyanatocadmate(II) complex in dimethyl sulfoxide (DMSO) has been studied by the EXAFS (extended X-ray absorption fine structure) and solution X-ray diffraction methods. It has been revealed that the tetrathiocyanatocadmate(II) complex has a five-coordinate structure with an additional DMSO molecule. The structure in DMSO is different from that in water and *N,N*-dimethylformamide, in which no solvent molecule coordinates to the central metal ion. It has also been seen that the coordination mode of the thiocyanate ions in the tetrathiocyanatocadmate(II) complex changes depending on the source of thiocyanate ions due, probably, to different hydrogen bonding abilities of the N- and S-sites of the thiocyanate ion with the counter cations, i.e., the $[Cd(NCS)_3(SCN)(dmso)]^{2-}$ and $[Cd(NCS)_4(dmso)]^{2-}$ complexes are formed in solutions containing NH_4SCN and $(C_2H_5)_4NSCN$, respectively. The Cd–N, Cd–S, and Cd–O bond lengths within $[Cd(NCS)_3(SCN)(dmso)]^{2-}$ are, respectively, 222(1), 262(1), and 234(1) pm, while the Cd–N and Cd–O bond lengths within $[Cd(NCS)_4(dmso)]^{2-}$ are 223(1) and 239(2) pm, respectively.

Zinc(II) and mercury(II) ions form N-coordinate $[Zn(NCS)_4]^{2-}$ and S-coordinate $[Hg(SCN)_4]^{2-}$ with thiocyanate ions, respectively, both in water and in dimethyl sulfoxide (DMSO).[1,2] As to cadmium(II), the N and S atoms of the thiocyanate ion bind to form $[Cd(NCS)_2(SCN)_2]^{2-}$ in water.[1,3] The bonding at N- and S-sites also occurs with a different coordination mode, $[Cd(NCS)_3(SCN)]^{2-}$, in *N,N*-dimethylformamide (DMF).[4] The different geometries around the cadmium(II) ion may be ascribed to different solvation tendencies of the thiocyanate ion in protic water and aprotic DMF.[4,5]

It is suggested from the Raman spectroscopic and calorimetric data that the coordination mode in the lower thiocyanato complexes of the cadmium(II) ion is $[Cd(NCS)]^+$, $[Cd(NCS)_2]$, and $[Cd(NCS)_2(SCN)]^-$ in DMF.[5] On the other hand, an X-ray diffraction study indicated that the cadmium(II) ion is coordinated with only sulfur atom of the thiocyanate ion in a DMSO solution containing the di- and trithiocyanato complexes.[2] The result suggests that the coordination structure of the higher cadmium(II) thiocyanato complexes is different in these solvents. Thus, we investigated the structure of the tetrathiocyanatocadmate(II) complex in DMSO. The X-ray diffraction method was first applied to the structure determination of the cadmium(II)-thiocyanate system after Persson, et al.[2] Furthermore, we employed the EXAFS (extended X-ray absorption fine structure) method for the system. Cadmium-113 NMR measurements were also carried out to obtain additional information on the coordination structure of the tetrathiocyanatocadmate(II) complex.

Experimental

Sample Solutions. All chemicals used were of reagent grade. Cadmium(II) perchlorate DMSO solvate was prepared by dissolving cadmium(II) perchlorate hydrate crystals in DMSO and recrystallized three times from DMSO and finally from acetone. Crystals thus obtained were dried at room temperature in a vacuum oven for several days. The analysis of the cadmium(II) perchlorate DMSO solvate by EDTA titration showed the composition of $Cd(ClO_4)_2(dmso)_6$. Cadmium(II) perchlorate DMF solvate and cadmium(II) thiocyanate were obtained by the same method as described elsewhere.[4] Ammonium thiocyanate and tetraethylammonium thiocyanate were dried at room temperature in vacuum. Dimethyl sulfoxide and *N,N*-dimethylformamide were purified as described elsewhere.[5,6]

Two sample solutions were prepared for X-ray diffraction measurements. Solution **A** was prepared by dissolving suitable amounts of cadmium(II) thiocyanate and ammonium thiocyanate in DMSO so as to involve the tetrathiocyanatocadmate(II) complex as the main species.[7] Solution **B** is an ammonium thiocyanate DMSO solution and is a reference sample in order to estimate the structure parameters of the tetrathiocyanatocadmate(II) complex present in solution **A**. Eight test solutions were prepared for EXAFS measurements. Solutions **AQ1**, **DMF1**, and **DMSO1** are the standard samples for a Cd–O atom pair containing the solvated cadmium(II) ion in water,[8] DMF,[4] and DMSO,[9] respectively, of known structure. Solutions **AQ2** and **DMF2** are also the structure standard for Cd–N and Cd–S atom pairs and involve the tetrathiocyanatocadmate(II) complex in water and DMF, respectively.[1,4] Three sample solutions, **DMSO2**, **DMSO3**, and **DMSO4**, were prepared by dissolving $Cd(SCN)_2$ along with either NH_4SCN or $(C_2H_5)_4NSCN$ in DMSO. In these solutions the tetrathiocyanatocadmate(II) complex is formed as the main species.[7] The composition of the sample solutions is given in Table 1.

X-Ray Diffraction Measurements. X-Ray diffraction data were obtained on a θ–θ type diffractometer (JEOL) and the Mo $K\alpha$ radiation (λ=71.07 pm) was used. The observed range of the scattering angle 2θ was from 2° to 140° and the data were recorded at least twice over the whole angle range. Details for X-ray diffraction measurements were described

Table 1. The Composition (mol dm^{-3}), Stoichiometric Volumes V, and Densities ρ of Sample Solutions[a)]

Solution	$Cd(SCN)_2$	NH_4SCN	DMSO	ρ/g cm^{-3}	$V/10^9$ pm^3	C_{SCN}/C_{Cd}
		X-Ray Diffraction Measurement				
A	0.6885	4.316	9.729	1.246	2.412	8.269
B	—	4.207	10.51	1.142	2.233	—
		EXAFS Measurement				
Solution	$Cd(ClO_4)_2$	$Cd(SCN)_2$	NH_4SCN	$(C_2H_5)_4NSCN$		C_{SCN}/C_{Cd}
AQ1	1.01	—	—	—		—
DMF1	0.850	—	—	—		—
DMSO1	0.694	—	—	—		—
AQ2	—	0.976	7.14	—		9.32
DMF2	—	0.938	4.21	—		6.49
DMSO2	—	0.689	4.27	—		8.19
DMSO3	—	0.200	—	1.14		7.70
DMSO4	—	0.100	—	1.00		12.0

a) C: Molar concentration of the ion indicated by the subscript.

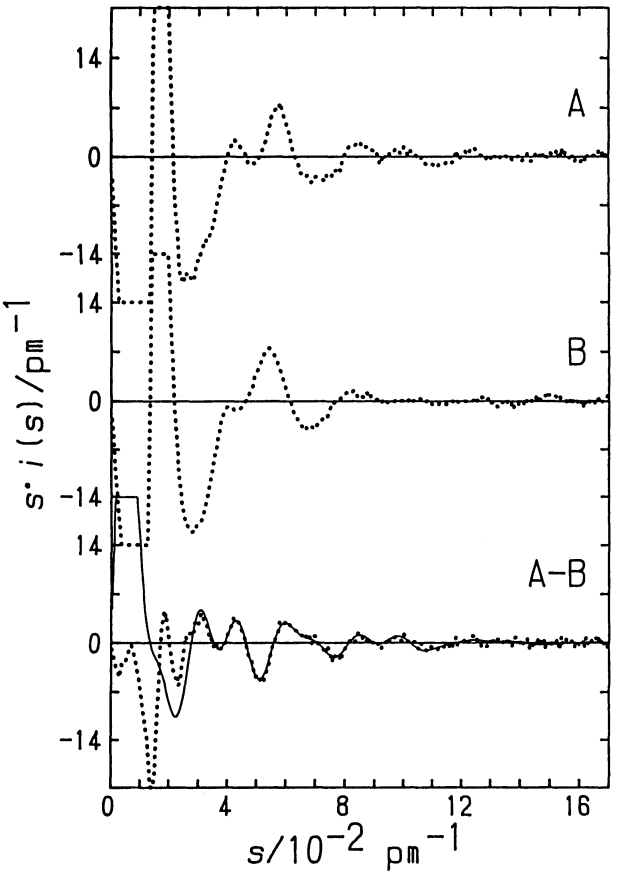

Fig. 1. The reduced intensities multiplied by s for solutions **A** and **B**, as well as the difference reduced intensities, **A**–**B**. The observed $s \cdot i(s)$ values are shown by dots and calculated ones by solid lines.

elsewhere.[10)]

The reduced intensities $i(s)$ were obtained as $\{K \cdot I(s) - \Sigma N_j \cdot f_j^2(s)\}$, where s ($=4\pi\lambda^{-1}\sin\theta$) represents the scattering vector and K a normalization factor of the observed intensities $I(s)$, which had been corrected for absorption, polarization, and multiple scattering of X-rays by a usual manner,[10)] to the absolute unit. N_j is the number of atom j in a stoichiometric volume V of sample solutions and $f_j(s)$ the atomic scattering factors at s of atom j corrected for anomalous dispersion. The reduced intensities multiplied by s for the sample solutions are depicted in Fig. 1.

The $s \cdot i(s)$ values are converted into the radial distribution function $D(r)$ as

$$D(r) = 4\pi r^2\rho_0 + \frac{2r}{\pi}\int_0^{s_{max}} s \cdot i(s) \cdot M(s) \cdot \sin(rs)ds. \quad (1)$$

$\rho_0 = \{\Sigma N_j \cdot f_j(0)\}^2 / V$ stands for the average scattering density in a stoichiometric volume and s_{max} the maximum s-value available in the measurement ($s_{max} = 16.6\times10^{-2}$ pm^{-1}). The modification function $M(s)$ has the form of $[\Sigma N_j \cdot f_j^2(0)/\Sigma N_j \cdot f_j^2(s)] \cdot \exp(-\kappa s^2)$, the damping factor κ being chosen as 100 pm^2 in the present case. Calculations were performed by using a program KURVLR.[11)]

The theoretical intensities $i(s)_{calcd}$ resulting from the interatomic interactions in the solutions are calculated as

$$i(s)_{calcd} = \sum_{\substack{p \\ p\neq q}}\sum_{q} n_{pq} f_p(s) f_q(s) \frac{\sin(r_{pq}s)}{r_{pq}s} \exp(-b_{pq}s^2), \quad (2)$$

where r_{pq}, b_{pq}, and n_{pq} stand for the distance, the temperature factor, and the frequency factor of the atom pair p–q, respectively. A least squares refinement for determining the structure parameters was carried out by comparing the observed and theoretical reduced intensities so as to minimize the error-square sum $U_1 = \Sigma s^2\{i(s)_{obsd} - i(s)_{calcd}\}^2$.

EXAFS Measurements. EXAFS spectra were measured around the Cd K-edge in the transmission mode using BL10B station at the Photon Factory of the National Laboratory for High Energy Physics.[12)] X-Rays were monochromatized by an Si(311) channel-cut crystal.

The apparent absorbance μx is obtained as $\ln(I_0/I)$, where I and I_0 are X-ray intensities with and without a sample, respectively. Both intensities I_0 and I were simultaneously measured by ionization chambers filled with Ar gas.

A glass fiber filter was immersed to sample solutions and then sealed in a Mylar bag in order to prevent evaporation of solvents. An effective jump at the absorption edge was obtained by changing the number of filters. Dilute solutions less than 0.2 mol dm^{-3} were held in a 1 cm thick Teflon cell with Mylar windows.

Background absorptions other than that for the K-edge of the cadmium atom were estimated by the least-squares fitting

with Victoreen formula[13] to the pre-edge and were subtracted from the total absorption by extrapolation. The smooth K-shell absorption μ_0 due to an isolated atom was evaluated by fitting a smooth curve to the observed absorption spectrum using a sixth-order polynomial function.

The EXAFS pattern $\chi(k)$ was then extracted and normalized as $\{\mu(k)-\mu_0(k)\}/\mu_0(k)$. k is the photoelectron wave vector ejected and given as $\{2m(E-E_0)\}^{1/2}/\hbar$. E represents the energy of the incident X-rays and E_0 is the threshold energy of a K-shell electron. The E_0 value was selected as the position of the half-height of the edge jump in each sample. The radial structure function $F(r)$ was obtained by the Fourier transformation of the $k^3\cdot\chi(k)$ values as

$$F(r)=(1/2\pi)^{1/2}\int_{k_{min}}^{k_{max}} k^3\cdot\chi(k)\cdot W(k)\cdot\exp(-2ikr)\mathrm{d}k. \quad (3)$$

$W(k)$ is a window function of the Hanning type.[14]

A curve fitting procedure in the k-space for the refinement of structure parameters was applied to the Fourier filtered $k^3\cdot\chi(k)_{obsd}$ values to minimize $U_2=\Sigma k^6\{\chi(k)_{obsd}-\chi(k)_{calcd}\}^2$. The model function $\chi(k)_{calcd}$ is given by the single-electron and single-scattering theory as[15-18]

$$\chi(k)_{calcd}=\Sigma\{n_j/(k\cdot r_j^2)\}\exp(-2\sigma^2k^2-2r_j/\lambda)F_j(\pi,k)\times\sin(2kr_j+\alpha_j(k)), \quad (4)$$

where $F_j(\pi, k)$ is the backscattering amplitude from each of n_j scatterers j at distance r_j from the X-ray absorbing atom. σ_j^2 is the mean square displacement of the equilibrium distance r_j and λ is the mean free path of a photoelectron ejected. $\alpha_j(k)$ is the total scattering phase shift experienced by the photoelectron. The values of $F_j(\pi, k)$ in Eq. 4 were quoted from the tables by Teo and Lee.[19] The phase shift $\alpha_j(k)$ was approximated by the function $a_0+a_1k+a_2k^2+a_3/k^3$,[20] where the coefficients a_0, a_1, a_2, and a_3 were evaluated by fitting the function to the theoretical phase shift values by Teo and Lee.[19] The E_0 value is usually treated as a parameter and evaluated from structure standards. The bond lengths between the cadmium(II) ion and ligand atoms in the standard samples examined in the present study were hardly reproducible by the refinement of the E_0 value. Therefore, the parameters a_0, a_1, and λ were determined from the standard sample of a known structure and then they were used as constants in the course of the structural analysis of unknown samples, while r, σ, and n values were optimized as variables.

NMR Measurements. Cadmium-113 NMR spectra were measured at 88.705 MHz by using a JEOL JNM-GX400 FT NMR spectrometer at the instrument center of the Institute for Molecular Science. Sample tubes of 10 mm diameter were used. The ^{113}Cd chemical shift in the aqueous $Cd(ClO_4)_2$ solution of 1.01 mol dm^{-3} was used as the standard; $\delta(Cd(ClO_4)_2)=0$ ppm.

Results and Discussion

X-Ray Diffraction. Figure 2 shows the radial distribution curves in the form of $D(r)-4\pi r^2\rho_0$ of solutions **A** and **B**, as well as the difference radial distribution curve obtained by subtraction of the $(D(r)-4\pi r^2\rho_0)$ curve of solution **B** from solution **A**, which will be discussed in the later section. Four main peaks are observed at 170, 250, 400, and 500 pm in the total radial distribution curves of solutions **A** and **B**. The first peak at 170 pm

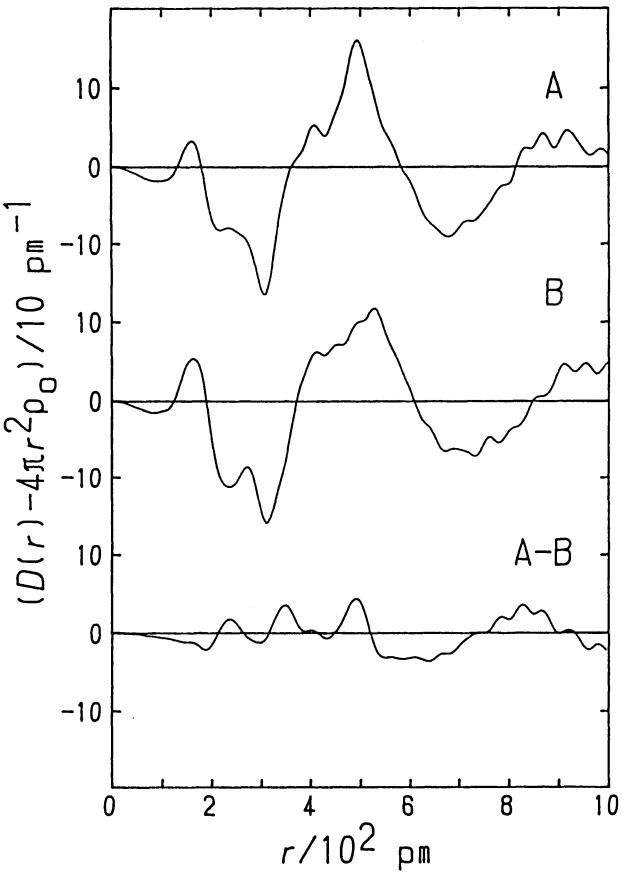

Fig. 2. The differential radial distribution functions, $D(r)-4\pi r^2\rho_0$, for solutions **A** and **B** and the difference radial distribution function, **A**–**B**.

is ascribed to the C–H, C–S, and S=O bonds within DMSO molecules and the N–H, C–S, and C≡N bonds within thiocyanate ions. The second peak around 250 pm is mainly originated from the nonbonding S···H and C···O pairs within DMSO molecules and the N···S pairs within thiocyanate ions. In the curve of solution **A** the bonds between cadmium(II) ion and ligand atoms within the tetrathiocyanatocadmate(II) ion may be included in the peak. According to an X-ray diffraction measurement of liquid DMSO,[21] a large and broad peak appears around 500 pm due to long-range intermolecular interactions among DMSO molecules. The third and fourth peaks with shoulders may mainly result from the intermolecular interactions of DMSO molecules, because these appear on a large and broad peak. Different peak shapes of the $D(r)$ curves in the range of 500 pm from that of liquid DMSO may be ascribed to the intermolecular interactions of ammonium and thiocyanate ions with DMSO molecules and structural changes in the liquid DMSO caused by various ion-solvent interactions. Such structural changes in liquid DMSO may lead to complications in the X-ray data analysis. Therefore, we took the difference between the two radial distribution curves (Fig. 2, **A**–**B**) in order to extract the structure information of the tetrathiocya-

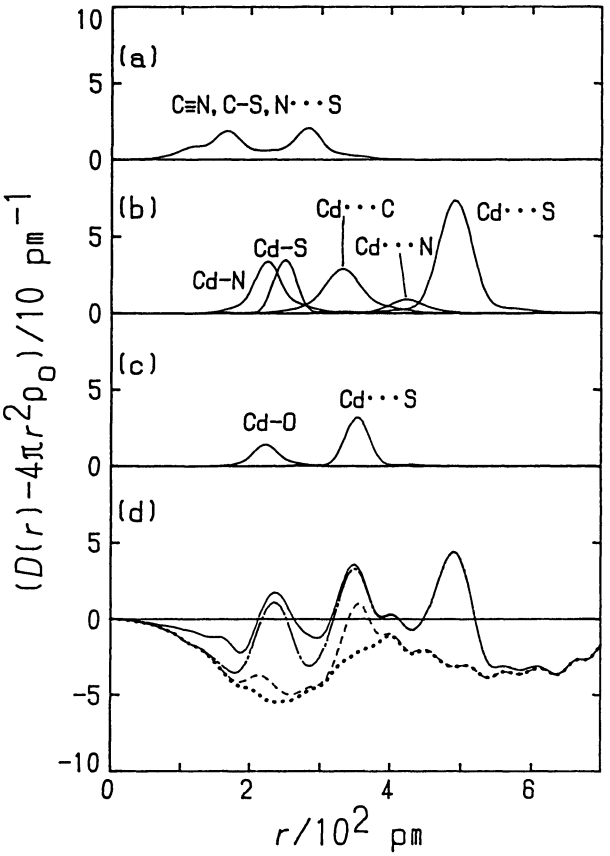

Fig. 3. The difference radial distribution curve. (a) The theoretical peak shapes for intramolecular interactions within ammonium and thiocyanate ions. (b) The peak shapes for the intramolecular interactions between cadmium(II) and thiocyanate within $[Cd(NCS)_3(SCN)(dmso)]^{2-}$. (c) The peak shapes for the interactions between cadmium(II) and DMSO. (d) The chain and dashed lines and dots represent the residual curves after subtraction of the theoretical peaks in (a), (a)+(b), and (a)+(b)+(c), respectively, from the original one (solid line).

natocadmate(II) complex, since the solutions have nearly the same concentrations of ammonium thiocyanate and DMSO.

Three main peaks were found below 600 pm in the difference radial distribution curve (Fig. 2, **A**–**B** and the solid line in Fig. 3d), which may mainly be ascribed to intramolecular interactions within the tetrathiocyanatocadmate(II) complex. The peaks at 230 and 350 pm in the curve may be ascribed to the Cd–N and Cd–S bonds and the nonbonding Cd···C pairs, respectively. The peak at 500 pm may be due to the nonbonding Cd···S pair between the cadmium(II) ion and sulfur atom of the N-bonding thiocyanate ion, and the peak area corresponds to approximately three Cd···S pairs as we have seen in the $[Cd(NCS)_3(SCN)]^{2-}$ complex in DMF.[4] Therefore, we may say that the structure of the tetrathiocyanatocadmate(II) ion is similar to that in DMF.[4] However, a small peak remaining at 230 pm (dashed line in Fig. 3d), which had not been seen in the DMF system, was not explainable by any combination of the lengths of three Cd–N and a Cd–S bonds. Moreover, the area of the peak at 350 pm was appreciably larger than that expected from the four Cd···C pairs within $[Cd(NCS)_3(SCN)]^{2-}$ and was reproducible by the assumption of an additional Cd···S pair. In fact, the peaks over the range of 200—400 pm were reasonably explained by the assumption of a DMSO molecule bound to the cadmium(II) ion, since Cd–O and Cd···S interactions should appear around 230 and 340 pm.[9] Subtraction of these peaks from the difference curve leads to a smooth background as seen in Fig. 3d (dotted line) over the range $r<400$ pm. From the analysis of the radial distribution curve, we concluded that the tetrathiocyanatocadmate(II) complex has a five-coordinate $[Cd(NCS)_3(SCN)(dmso)]^{2-}$ structure with a DMSO molecule. A five-coordinate structure of several cadmium(II) complexes has so far been reported for

Table 2. Results of the Least-Squares Refinements for the Structure Parameters of the Tetrathiocyanatocadmate(II) Complex by Using the Difference Reduced Intensities[a]

Model	Interaction	r/pm	b/10 pm^2	n
$[Cd(NCS)_3(SCN)(dmso)]^{2-}$	Cd–N(SCN$^-$)	223(5)	3(5)	3[b]
U_1=3.87×10^5	Cd–S(SCN$^-$)	249(7)	1(7)	1[b]
	Cd···C(SCN$^-$)	327[c]	15[b]	3[b]
	Cd···C(SCN$^-$)	334[d]	15[b]	1[b]
	Cd···N(SCN$^-$)	423[d]	14[b]	1[b]
	Cd···S(SCN$^-$)	491(1)	14(2)	3[b]
	Cd–O(dmso)	221(10)	2(8)	1[b]
	Cd···S(dmso)	352(2)	3(2)	1[b]
$[Cd(NCS)_3(SCN)]^{2-}$	Cd···N(SCN$^-$)	220(1)	−2(1)	3[b]
U_1=8.54×10^5	Cd···S(SCN$^-$)	245(1)	−3(1)	1[b]
	Cd···C(SCN$^-$)	324[c]	15[b]	3[b]
	Cd···C(SCN$^-$)	331[d]	15[b]	1[b]
	Cd···N(SCN$^-$)	420[d]	14[b]	1[b]
	Cd···S(SCN$^-$)	489(1)	11(2)	3[b]

a) Standard deviations are given in parentheses. b) The values were kept constant during the calculations. c) ∠Cd–N–C=148° is assumed (Ref. 1). d) ∠Cd–S–C=∠Cd–S–N=106° is assumed (Ref. 1).

Table 3. Cadmium-113 NMR Chemical Shifts of the Tetrathiocyanatocadmate(II) Complexes in Water, DMF, and DMSO

Solution	Species	Chemical shift/ppm
AQ1	$[Cd(H_2O)_6]^{2+}$ in water	0
AQ2	$[Cd(NCS)_2(SCN)_2]^{2-}$ in water	206
DMF2	$[Cd(NCS)_3(SCN)]^{2-}$ in DMF	220
DMSO2	$[Cd(NCS)_3(SCN)(dmso)]^{2-}$ in DMSO	138

dichloro(2-pyridinecarbaldehyde 2-pyridylhydrazone)-cadmium(II), dithiocyanato(tri-*m*-tolylphosphine)cadmium(II), tetrakis(μ-trifluoroacetato)bis[(triphenylphosphine)cadmium(II)], etc.[22–27] The five-coordinate structure of the $[Cd(NCS)_3(SCN)(dmso)]^{2-}$ complex has been confirmed by the EXAFS measurements as we will discuss in the later section.

The structure parameters were refined by a least-squares calculation using the $s \cdot i(s)$ values in the difference curve in the high angle region ($s > 4\times10^{-2}$ pm^{-1}). The structure models examined were the four-coordinate $[Cd(NCS)_3(SCN)]^{2-}$ and five-coordinate $[Cd(NCS)_3(SCN)(dmso)]^{2-}$ ions. In the fitting procedures, the interactions of the central cadmium(II) ion with thiocyanate ions and a DMSO molecule in the coordination sphere were taken into consideration. Since the contribution of the nonbonding Cd···C and Cd···N pairs to the difference reduced intensity values is rather small, the lengths of the bonds were calculated from the Cd–S–C, Cd–N–C, and Cd–S–N bond angles found in an aqueous solution.[1] The structure parameters thus obtained are listed in Table 2. As seen in the table an assumption of the five-coordinate $[Cd(NCS)_3(SCN)(dmso)]^{2-}$ structure gave a smaller error-square sum than that of the four-coordinate $[Cd(NCS)_3(SCN)]^{2-}$. Moreover, the temperature factors of the Cd–N and Cd–S bonds are unreasonably negative in the latter model.

NMR. In Table 3 are summarized the ^{113}Cd NMR chemical shifts of the tetrathiocyanatocadmate(II) complexes in water, DMF, and DMSO. According to an ab initio theoretical study, the change in the ^{113}Cd chemical shifts is very sensitive to the paramagnetic contribution to the shielding constant and thus the shifts mainly reflect the electron donating ability of ligands and increase with increasing the electron donating ability of ligands.[28] In fact, the shielding of ^{113}Cd has been found to increase in the order O<N<S for many cases.[29–33] The cadmium-113 resonance listed in Table 3 shifts downfield upon the formation of the tetrathiocyanatocadmate(II) complexes in water, DMF, and DMSO, and the direction of the shifts qualitatively agrees with the fact that the ligation of nitrogen and sulfur occurs instead of oxygen. Although these shifts cannot be quantitatively interpreted on the basis of the simple electron donating ability of ligating atoms, the slightly different chemical shifts in water and DMF may be ascribed to the different coordination mode of thiocyanate ion, i.e., $[Cd(NCS)_2(SCN)_2]^{2-}$ in water and $[Cd(NCS)_3(SCN)]^{2-}$ in DMF. A similar chemical shift to that in DMF may be expected for the tetrathiocyanatocadmate(II) complex in DMSO if the complex had the four-coordination $[Cd(NCS)_3(SCN)]^{2-}$ structure like in DMF. However, the cadmium-113 resonance of the DMSO solution appreciably shifts upfield relative to that of DMF. The result agreed with that of the X-ray diffraction measurement in which we found that the coordination number of the cadmium(II) ion in the tetrathiocyanato complex is larger in DMSO than in DMF but smaller than that in the $[Cd(H_2O)_6]^{2+}$ complex in water.

EXAFS. Figure 4 depicts the extracted EXAFS oscillations weighted by k^3 of the sample solutions. The Fourier transforms of the sample solutions are shown in Fig. 5 (uncorrected for the phase shift). The first intense peaks appearing at 150—200 pm in the

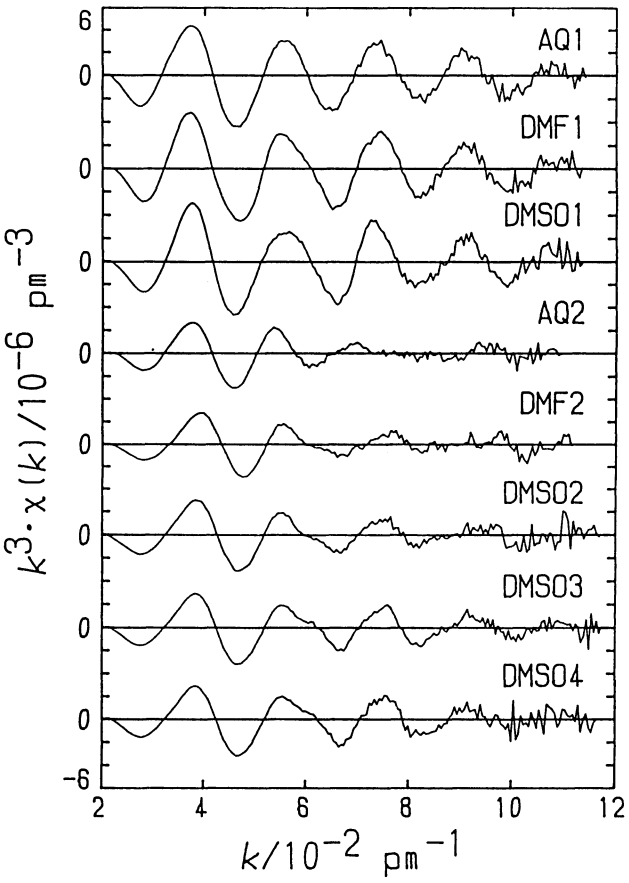

Fig. 4. The extracted EXAFS oscillations in the form of $k^3 \cdot \chi(k)$ for sample solutions.

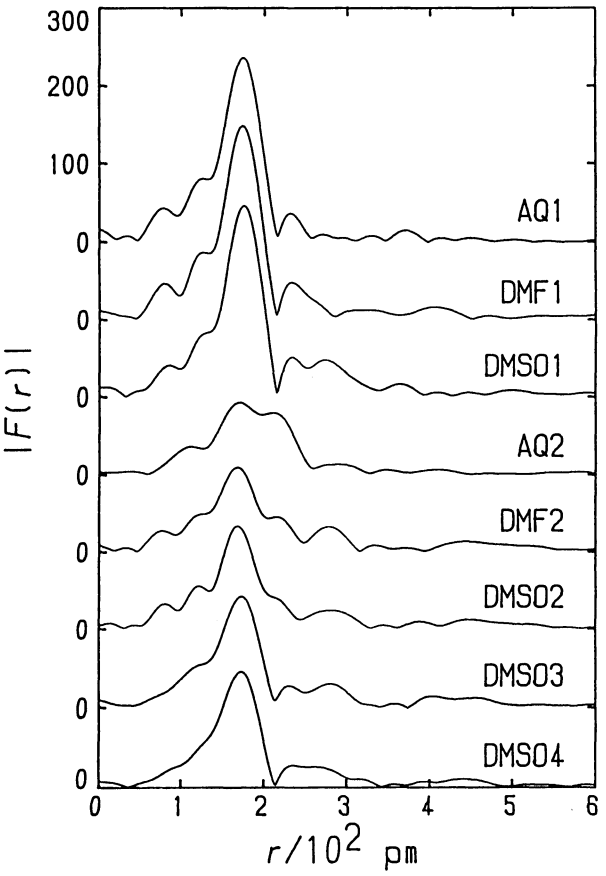

Fig. 5. The radial structure functions $|F(r)|$ for sample solutions, phase shift uncorrected.

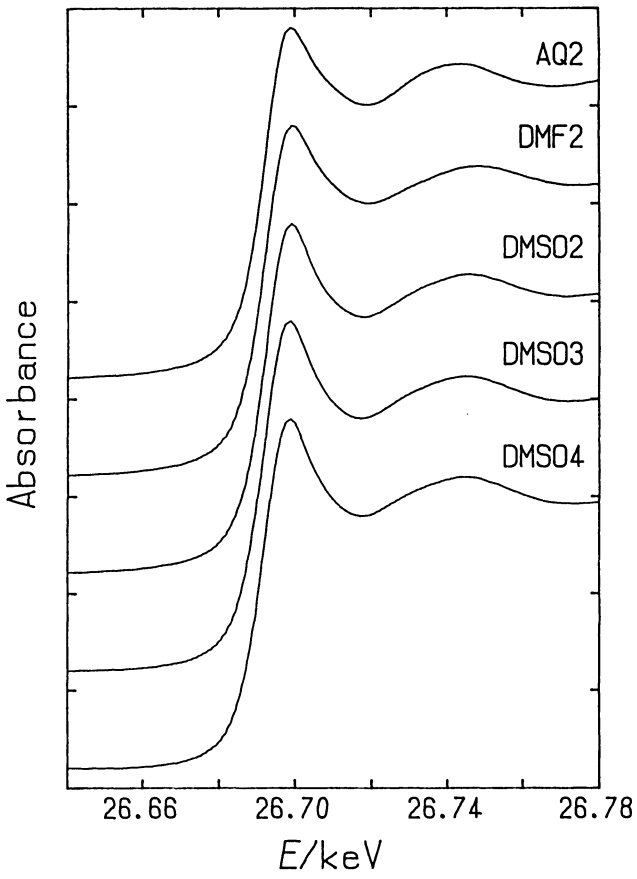

Fig. 6. The X-ray absorption spectra in the near edge region for sample solutions containing the tetrathiocyanatocadmate(II) complex.

figure are due to the bonds between the cadmium(II) ion and oxygen, nitrogen, and sulfur atoms in the first coordination sphere of the cadmium(II) ion. The peak shape of solutions **AQ1**, **DMF1**, and **DMSO1** is virtually the same because the solutions involve the six-coordinate octahedral CdO_6 moiety[4,8,9] The peak shape drastically changed in solutions **AQ2** and **DMF2** upon formation of the tetrathiocyanatocadmate(II) ion. The different peak shapes between solutions **AQ2** and **DMF2** are ascribed to different coordination geometries around the cadmium(II) ion, i.e., $[Cd(NCS)_2(SCN)_2]^{2-}$ in water and $[Cd(NCS)_3(SCN)]^{2-}$ in DMF.[1,4] For **DMSO2**, **DMSO3**, and **DMSO4** containing the tetrathiocyanatocadmate(II) complex, the peak shapes are different from those in water and DMF. The peak height of **DMSO2** and those of **DMSO3** and **DMSO4** are 20% and 30%, respectively, larger than that of solution **DMF2**. This result shows that the coordination structure of the tetrathiocyanatocadmate(II) ion in DMSO is different from that in water and DMF, consistent with the finding from the X-ray diffraction and ^{113}Cd NMR measurements discussed in the previous sections. Moreover, the peak shape of **DMSO2** is different from that of **DMSO3** and **DMSO4**, suggesting that the structure of the complex changes depending on the source of thiocyanate ions.

Figure 6 shows the X-ray absorption spectra in the near edge region of cadmium atom for the sample solutions involving the tetrathiocyanatocadmate(II) complex. In each spectrum absorbances were normalized by the respective edge jump. The spectral shapes are different for all solutions except for the spectra of **DMSO3** and **DMSO4**. The different absorption pattern may reflect the different multiple scattering processes caused by the different symmetries and/or different neighboring atoms around the cadmium(II) ion, i.e., the different coordination structures of the tetrathiocyanatocadmate(II) complex in different *solvents*. Thus, the coordination structure of the tetrathiocyanatocadmate(II) complex in DMSO is different from that in water and DMF and also changes depending on the source of thiocyanate ions.

The structure parameters of complexes were finally determined by a curve fit in the k-space using the Fourier filtered $k^3 \cdot \chi(k)$ values, which were obtained by the inverse transformation of the $F(r)$ curve over the r-range including the main peak for each sample. A least-squares calculation was applied over the range $4 < k/10^{-2}\ pm^{-1} < 10$. The phase function and the λ value for a Cd–O atom pair were first evaluated from solutions **AQ1**, **DMF1**, and **DMSO1** containing the octahedrally solvated cadmium(II) ions of the known

Table 4. Results of the Least-Squares Refinements for Standard Samples[a]

Type	Interaction	r/pm	σ/pm	n	U_2	r_{X-ray}/pm
		$[Cd(H_2O)_6]^{2+}$ in water (Solution **AQ1**)				
I	Cd–O	231(1)	8.0(2)	6[b]	3.45	231[c]
II	Cd–O	231(1)	8[b]	6[b]	3.85	231[c]
		$[Cd(dmf)_6]^{2+}$ in DMF (Solution **DMF1**)				
I	Cd–O	230(1)	7.9(2)	6[b]	2.30	229.8[d]
II	Cd–O	230(1)	8[b]	6[b]	2.33	229.8[d]
		$[Cd(dmso)_6]^{2+}$ in DMSO (Solution **DMSO1**)				
I	Cd–O	230(1)	7.9(1)	6[b]	1.93	229.4[e]
II	Cd–O	230(1)	8[b]	6[b]	1.96	229.4[e]
		$[Cd(NCS)_2(SCN)_2]^{2-}$ in water (Solution **AQ2**)				
I	Cd–N	226(1)	7.3(3)	2[b]	2.65	224.6[f]
	Cd–S	264(1)	9.5(2)	2[b]		264.9[f]
II	Cd–N	226(1)	8[b]	2[b]	3.91	224.6[f]
	Cd–S	263(1)	9[b]	2[b]		264.9[f]
		$[Cd(NCS)_3(SCN)]^{2-}$ in DMF (Solution **DMF2**)				
I	Cd–N	221(1)	8.2(1)	3[b]	1.06	223[d]
	Cd–S	258(1)	8.7(6)	1[b]		257[d]
II	Cd–N	221(1)	8[b]	3[b]	1.41	223[d]
	Cd–S	258(1)	9[b]	1[b]		257[d]

a) The values in parentheses represent standard deviation. b) The values were kept constant during the calculations. c) Ref. 13. d) Ref. 4. e) Ref. 14. f) Ref. 1.

Table 5. Results of the Least-Squares Refinements for Solution **DMSO2**[a]

Model	Interaction	r/pm	σ/pm	n	U_2
$[Cd(NCS)_3(SCN)]^{2-}$	Cd–N	232.3(2)	8[b]	3[b]	3.72
	Cd–S	258.7(6)	9[b]	1[b]	
$[Cd(NCS)_4]^{2-}$	Cd–N	225.1(3)	8[b]	4[b]	19.85
$[Cd(NCS)_3(SCN)(dmso)]^{2-}$	Cd–N	221.6(1)	8[b]	3[b]	2.67
	Cd–S	261.5(5)	9[b]	1[b]	
	Cd–O	233.9(7)	8[b]	1[b]	
$[Cd(NCS)_4(dmso)]^{2-}$	Cd–N	223.3(3)	8[b]	4[b]	7.48
	Cd–O	245(1)	8[b]	1[b]	
$[Cd(NCS)_3(SCN)(dmso)_2]^{2-}$	Cd–N	219.4(3)	8[b]	3[b]	6.76
	Cd–S	264.1(5)	9[b]	1[b]	
	Cd–O	235.0(5)	8[b]	2[b]	
$[Cd(NCS)_4(dmso)_2]^{2-}$	Cd–N	221.3(2)	8[b]	4[b]	4.31
	Cd–O	242.6(6)	8[b]	2[b]	

a) The values in parentheses represent standard deviation, which have been estimated from three independent measurements. b) The values were kept constant during the calculations.

Table 6. Results of the Least-Squares Refinements for Solution **DMSO3**[a]

Model	Interaction	r/pm	σ/pm	n	U_2
$[Cd(NCS)_3(SCN)]^{2-}$	Cd–N	222.8(6)	8[b]	3[b]	13.48
	Cd–S	252(1)	9[b]	1[b]	
$[Cd(NCS)_4]^{2-}$	Cd–N	224(1)	8[b]	4[b]	3.67
$[Cd(NCS)_3(SCN)(dmso)]^{2-}$	Cd–N	223(4)	8[b]	3[b]	10.53
	Cd–S	259(2)	9[b]	1[b]	
	Cd–O	226(9)	8[b]	1[b]	
$[Cd(NCS)_4(dmso)]^{2-}$	Cd–N	222.5(4)	8[b]	4[b]	1.93
	Cd–O	239.2(8)	8[b]	1[b]	
$[Cd(NCS)_3(SCN)(dmso)_2]^{2-}$	Cd–N	220.4(5)	8[b]	3[b]	15.89
	Cd–S	268(2)	9[b]	1[b]	
	Cd–O	232.5(9)	8[b]	2[b]	
$[Cd(NCS)_4(dmso)_2]^{2-}$	Cd–N	220.7(4)	8[b]	4[b]	5.62
	Cd–O	238.3(7)	8[b]	2[b]	

a) The values in parentheses represent standard deviation, which have been estimated from three independent measurements. b) The values were kept constant during the calculations.

Table 7. Results of the Least-Squares Refinements for Solution **DMSO4**[a]

Model	Interaction	r/pm	σ/pm	n	U_2
$[Cd(NCS)_3(SCN)]^{2-}$	Cd–N	223.0(4)	8[b]	3[b]	16.21
	Cd–S	249(2)	9[b]	1[b]	
$[Cd(NCS)_4]^{2-}$	Cd–N	224.1(3)	8[b]	4[b]	3.51
$[Cd(NCS)_3(SCN)(dmso)]^{2-}$	Cd–N	224(4)	8[b]	3[b]	12.01
	Cd–S	257(4)	9[b]	1[b]	
	Cd–O	225(12)	8[b]	1[b]	
$[Cd(NCS)_4(dmso)]^{2-}$	Cd–N	222.4(3)	8[b]	4[b]	0.83
	Cd–O	238(1)	8[b]	1[b]	
$[Cd(NCS)_3(SCN)(dmso)_2]^{2-}$	Cd–N	220.5(4)	8[b]	3[b]	12.01
	Cd–S	273(5)	9[b]	1[b]	
	Cd–O	233(2)	8[b]	2[b]	
$[Cd(NCS)_4(dmso)_2]^{2-}$	Cd–N	220.5(3)	8[b]	4[b]	4.80
	Cd–O	237.4(9)	8[b]	2[b]	

a) The values in parentheses represent standard deviation, which have been estimated from three independent measurements. b) The values were kept constant during the calculations.

structure.[4,8,9] The phase functions for Cd–N and Cd–S atom pairs were then estimated from **AQ2** and **DMF2** involving the tetrathiocyanatocadmate(II) complexes,[1,4] the λ value being kept constant at the value determined from the standard Cd–O pair. The σ values for the Cd–O, Cd–N, and Cd–S bonds were also optimized as variables, while the Cd–O, Cd–N, and Cd–S bond lengths and numbers of the relevant interactions were kept at the literature values in the fitting procedures. The reproducibility of the bond lengths in the respective complexes were finally examined by adopting the λ value and phase functions thus evaluated. The results are summarized in Table 4 (type-I calculation). The bond lengths within the respective complexes agreed well with those determined by X-ray diffraction, and thus the phase functions were evaluated by the present analysis with reasonable certainties.

The interatomic distances and Debye–Waller factors of the bonds within the tetrathiocyanatocadmate(II) complex in DMSO were refined at the next step of the curve-fit analysis. On the basis of the result from the X-ray scattering data, three kinds of the bonds, Cd–N, Cd–O, and Cd–S, within the tetrathiocyanatocadmate(II) complex should be taken into consideration in the least-squares calculations. The reliability of the structure parameters to be determined is relatively low in such a three-shell fit due to strong correlations of the bond lengths with the Debye–Waller factors. Accordingly, the number of structure parameters to be optimized was reduced on the basis of a reasonable assumption. Here, the Debye–Waller factors for the Cd–O, Cd–N, and Cd–S bonds were fixed at the given values in Table 4 (type-II calculation) in the course of calculations, the values being the averaged ones for relevant interactions in the type-I calculation. As seen in Table 4, the bond lengths are well reproduced even by setting constraint on the Debye–Waller factors.

Various structure models for the tetrathiocyanatocadmate(II) complex in DMSO were examined in the least-squares calculation for the determination of the bond lengths. The structure models covered four-coordinate $[Cd(NCS)_3(SCN)]^{2-}$ and $[Cd(NCS)_4]^{2-}$, five-coordinate $[Cd(NCS)_3(SCN)(dmso)]^{2-}$ and $[Cd(NCS)_4(dmso)]^{2-}$, and six-coordinate $[Cd(NCS)_3(SCN)(dmso)_2]^{2-}$ and $[Cd(NCS)_4(dmso)_2]^{2-}$. The results for **DMSO2**, **DMSO3**, and **DMSO4** are summarized in Tables 5, 6, and 7, respectively. In the ammonium thiocyanate solution (**DMSO2**, see Table 5), the calculated $k^3 \cdot \chi(k)$ values based on the $[Cd(NCS)_3(SCN)(dmso)]^{2-}$ model

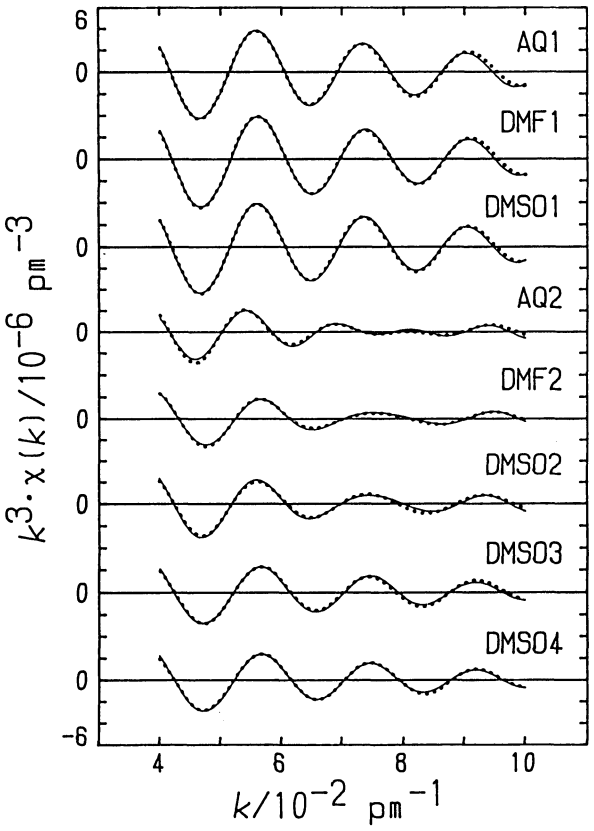

Fig. 7. The Fourier filtered $k^3 \cdot \chi(k)$ curves of the main peak shown in Fig. 5. The observed ones are shown by dots and the calculated ones by solid lines.

gave the best agreement with the observed ones, consistent with the result from the X-ray diffraction measurement. On the other hand, the least-squares refinement derived a conclusion that all thiocyanate ions coordinated to the cadmium(II) ion via N-atoms in the tetraethylammonium thiocyanate DMSO solutions (**DMSO3** and **DMSO4**), because the $[Cd(NCS)_4(dmso)]^{2-}$ model gave the smallest error-square sum (see Tables 6 and 7). The Cd–O bond lengths thus obtained lie within a reasonable range expected from the sum of the size of a cadmium(II) ion and an oxygen atom. Therefore, we concluded that a DMSO molecule coordinated to the cadmium(II) ion to form the five-coordinated tetrathiocyanatocadmate(II) complex in DMSO. In Fig. 7 we show the agreements between experimental and calculated $k^3 \cdot \chi(k)$ curves.

Conclusions

The tetrathiocyanatocadmate(II) complex in DMSO has a five-coordinate structure and is described as $[Cd(NCS)_3(SCN)(dmso)]^{2-}$ in the ammonium thiocyanate DMSO solution and as $[Cd(NCS)_4(dmso)]^{2-}$ in the tetraethylammonium thiocyanate solution. The different coordination geometries around the cadmium(II) ion with different medium electrolytes may be ascribed to different hydrogen-bonding abilities of the N- and S-sites of the thiocyanate ion with the counter cations. The thiocyanate ion may interact with ammonium ions through the N-site, and thus some of the SCN^- ions in the coordination shell turn outside the sphere to interact with NH_4^+ ions. However, since the tetraethylammonium ion does not form any hydrogen bonds with N- and S-sites, all SCN^- ions in the coordination sphere tend to orient towards the central cadmium(II) ion in the tetraethylammonium solution at the formation of the tetrathiocyanatocadmate(II) complex.

The tetrathiocyanatocadmate(II) ion has a five- and four-coordination structures in DMSO and DMF, respectively. DMSO has a slightly larger coordination ability than DMF, but the difference between them seen in terms of the donor number may not be so significant to explain the different coordination structures of the complexes in the solvents.[34,35] One of the plausible explanations for the different coordination geometries may be inter-ligand interactions between a thiocyanate ion and a DMSO molecule in the coordination sphere of the cadmium(II) ion. When we construct a model structure of the five-coordinate tetrathiocyanatocadmate(II) ion, lone pair electrons in the sulfur atom of the DMSO molecule direct towards the carbon atom of an adjacent N-bonded thiocyanate ion. An extra stabilization energy may thus be obtained from the favorable ligand-ligand interaction between an SCN^- ion and a DMSO molecule in the coordination sphere.

The authors thank Dr. Kiyohiko Nakajima of the Institute for Molecular Science for his kind help in the ^{113}Cd NMR measurements. EXAFS measurements have been performed under the approval of the Photon Factory Program Advisory Committee (Proposal No. 89-131).

References

1) T. Yamaguchi, K. Yamamoto, and H. Ohtaki, *Bull. Chem. Soc. Jpn.*, **58**, 3235 (1985).
2) I. Persson, Å. Iverfeldt, and S. Ahrland, *Acta Chem. Scand., Ser. A*, **35**, 295 (1981).
3) S. Ishiguro, K. Yamamoto, and H. Ohtaki, *Bull. Chem. Soc. Jpn.*, **59**, 1009 (1986).
4) K. Ozutsumi, T. Takamuku, S. Ishiguro, and H. Ohtaki, *Bull. Chem. Soc. Jpn.*, **62**, 1875 (1989).
5) S. Ishiguro, T. Takamuku, and H. Ohtaki, *Bull. Chem. Soc. Jpn.*, **61**, 3901 (1988).
6) S. Ishiguro, H. Suzuki, B. G. Jeliazkova, and H. Ohtaki, *Bull. Chem. Soc. Jpn.*, **59**, 2407 (1986).
7) S. Ishiguro, T. Takamuku, K. Ozutsumi, and H. Ohtaki, to be published.
8) H. Ohtaki, M. Maeda, and S. Ito, *Bull. Chem. Soc. Jpn.*, **47**, 2217 (1974).
9) M. Sandström, I. Persson, and S. Ahrland, *Acta Chem. Scand., Ser. A*, **32**, 607 (1978).
10) H. Ohtaki, *Rev. Inorg. Chem.*, **4**, 103 (1982).
11) G. Johansson and M. Sandström, *Chem. Scr.*, **4**, 195 (1973).
12) M. Nomura, "KEK Report 85-7," National Laboratory for High Energy Physics, Tsukuba, Japan, 1985.
13) "International Tables for X-Ray Crystalloaraphy," Kynoch Press, Birmingham, England (1962), Vol. III, p. 161.
14) F. J. Harris, *Proc. IEEE*, **66**, 51 (1978).
15) D. E. Sayers, E. A. Stern, and F. W. Lytle, *Phys. Rev. Lett.*, **27**, 1204 (1971).
16) E. A. Stern, *Phys. Rev. B*, **10**, 3027 (1974).
17) E. A. Stern, D. E. Sayers, and F. W. Lytle, *Phys. Rev. B*, **11**, 4836 (1975).
18) B. Lengler and P. Eisenberger, *Phys. Rev. B*, **21**, 4507 (1980).
19) B.-K. Teo and P. A. Lee, *J. Am. Chem. Soc.*, **101**, 2815 (1979).
20) P. A. Lee, B.-K. Teo, and A. L. Simons, *J. Am. Chem. Soc.*, **99**, 3856 (1977).
21) H. Ohtaki and S. Itoh, *Z. Naturforsch., A*, **42**, 858 (1979).
22) G. M. C. Higgins and B. Saville, *J. Chem. Soc.*, **1963**, 2812.
23) F. Lions, I. G. Dance, and J. Lewis, *J. Chem. Soc. A*, **1967**, 565.
24) R. G. Goel, W. P. Henry, M. J. Olivier, and A. L. Beauchamp, *Inorg. Chem.*, **20**, 3924 (1981).
25) T. Allman, R. C. Goel, N. K. Jha, and A. L. Beauchamp, *Inorg. Chem.*, **23**, 914 (1984).
26) S. Lacelle, W. C. Stevens, D. M. Kurtz, Jr., and J. W. Richardson, Jr., *Inorg. Chem.*, **23**, 930 (1984).
27) H. Strasdeit, W. Saak, S. Pohl, W. L. Driessen, and J. Reedijk, *Inorg. Chem.*, **27**, 1557 (1988).
28) H. Nakatsuji, K. Kanda, K. Endo, and T. Yonezawa, *J. Am. Chem. Soc.*, **106**, 4653 (1984).
29) M. Munakata, S. Kitagawa, and F. Yagi, *Inorg. Chem.*, **25**, 964 (1986).
30) C. F. Jensen, S. Deshmukh, H. J. Jakobsen, R. R.

Inners, and P. D. Ellis, *J. Am. Chem. Soc.*, **103**, 3659 (1981).
31) G. K. Carson, P. A. W. Dean, and M. Stillman, *Inorg. Chim. Acta,* **56**, 59 (1981).
32) R. A. Haberkorn, L. Que, W. O. Gillum, R. H. Holm, C. S. Liu, and R. C. Lord, *Inorg. Chem.*, **15**, 2408 (1976).
33) A. D. Cardin, P. D. Ellis, J. D. Odom, and J. W. Howard, *J. Am. Chem. Soc.*, **97**, 1672 (1975).
34) J. A. Riddick, W. B. Bunger, and T. K. Sakamoto, "Organic Solvents," 4th ed, Wiley-Interscience, New York (1986).
35) V. Gutmann, "The Donor-Acceptor Approach to Molecular Interactions," Plenum, New York (1971).